5 Scanning Probes for the Life Sciences

Andrea M. Ho · Horacio D. Espinosa

Abstract. Scanning probe based patterning techniques have the unique ability to deposit biological material into specific architectures on substrates and read and analyze the patterns using an atomic force microscope. Such devices are able to make much smaller biomolecule patterns, on the order of nanometers, than conventional techniques such as microcontact printing and optical lithography. A reduction in patterned feature size allows for greater sensitivity in biological studies and in life sciences applications such as drug screening and immunoassays. A variety of tools for the fabrication of nanoarrays are discussed. These include open- and closed-channel devices and pipette-based devices. Their potential for the integration of active components or augmentation to large-scale arrays for high-throughput deposition are examined. The mechanisms for deposition and biomolecule transport are also explained.

Key words: Nanoarrays, Patterning, Atomic force microscopy, Dip-pen nanolithography, Fountain probe, Protein array, Water meniscus

5.1 Introduction

In recent years novel techniques for depositing very small amounts of material, on the order of picoliters or less, onto surfaces at precise locations have been developed. While such efforts are clearly relevant in the fabrication of miniature electronics devices, it is now apparent that such techniques have many applications in biology and the life sciences as well. For example, the ability to spatially orient and immobilize biomolecules on a solid substrate is useful in the development of genomic or proteomic profiles of cells, drug screening, as well as biosensing, which requires precise and high-density arrays of biological material. Because cell functions are often mediated by the binding of a ligand to its membrane receptor, the study of cellular functions of living cells at the nanometer scale requires a device capable of delivering proteins to a particular location at a specific time [1]. This must be followed by an observation of the response.

In the design of a biomolecule-patterning device it is necessary to consider a multitude of factors. These include its resolution—the minimum feature size that can be patterned on the substrate; its reproducibility—small features must be repeatable and reliably patterned; and its ability for precise positioning. For use in high-throughput applications, a device should be easily scalable, i.e., its design should enable it to pattern arrays of biological material on the scale of a few centimeters. Devices that could deliver multiple solutions would have the advantage of depositing different

molecules within one set of nanostructures spaced nanometers apart. For applications in the life sciences, a device must be able to function in ambient conditions. Finally, the ability to verify the successful deposition of biological material is also useful.

A key aspect in nanopatterning is the careful control of substrate surface chemistry. Nonspecific binding must be avoided otherwise intended signals will be masked in biosensing applications. Protein patterns must also be stable because in biosensors or bioanalytical devices immobilized proteins are often rinsed or washed with water, buffer solutions or surfactants [2]. This can be controlled by an appropriate choice of interactions used for immobilization. Immobilization via electrostatic interactions is normally reversible; proteins may be removed using certain buffers or surfactants. For long-term stability, covalent binding, which involves the formation of disulfide, imine or amide bonds, is often used.

In this chapter we review micro and nano patterning technologies with a particular emphasis on bioapplications. We begin by looking at microscale techniques for DNA and protein studies and then proceed to a review of nanoscale technologies, focusing on probe-based device designs and patterning results. The theoretical aspects behind nanoscale deposition is discussed followed by an overview of advances in the parallelization of the aforementioned devices.

5.2 Microarray Technology

Molecular spot arrays can be used for massively parallel determination and measurements of binding events and open up possibilities for automation. A major benefit of microarrays and nanoarrays is that they require only minute amounts of sample material. In essence, microarrays consist of many microscopic spots, each containing identical molecules, attached to a solid support. In a typical microarray experiment, or immunoassay, these spots contain one binding partner, such as a receptor or ligand. A sample containing targets to be investigated is then added to the array, and binding between the probe spots and the targets may occur. Fluorescent labels are often used to detect such binding events. DNA is likely the most interesting biomolecule because of its role in information storage [3]. Its stability also makes it useful in directing the immobilization and assembly of nanostructures. Patterned in arrays, DNA can be used as probes to analyze genetic defects and single nucleotide polymorphisms using lab-on-a-chip approaches.

There are two main methods for microarray production. The first involves synthesis on the chip to create libraries of short oligonucleotides (short sequences of nucleotides, the structural units of DNA and RNA) or peptides (compounds of two or more amino acids). This may be accomplished using techniques such as optical lithography. The second method involves separate synthesis with subsequent deposition on the chip, which is required for larger biomolecules such as polynucleotides or proteins. This type of deposition has been accomplished with restricted reproducibility via contact printing using pin tools dipped into a sample solution and brought into contact with the support material, thereby dispensing the solution. Optical lithography and microcontact printing will be discussed in greater detail in the following section. The experimental variability using microspotting techniques

is expected to decrease with the recent advances being made [4]. Other devices are noncontact equipment such as inkjet printers which use the piezo effect to deposit nanoliter volumes of solution [3]. The distance between deposited drops has been minimized to 200 μm, resulting in arrays that are not very dense. Nevertheless, inkjet methods allow for in situ synthesis and can therefore deposit longer oligonucleotides than methods such as photolithography. Longer oligonucleotides offer sufficient specificity to detect genes using fewer probes [5].

5.2.1 Microcontact Printing

Microcontact printing is one method used to create microarrays. The technique covers an existing patterned surface, the master, with a liquid prepolymer. This is then cured to create an elastomeric stamp [6]. Typically, poly(dimethylsiloxane) (PDMS) is used. The hardened stamp is then peeled off the master. Ink solution is applied, the solvent is allowed to evaporate and the stamp is brought into contact with a substrate, at which point the ink is transferred. The ink forms a self-assembled monolayer (SAM) which is a replica of the master pattern.

Microcontact printing was first introduced by Whitesides and coworkers in 1993 as an alternative to photolithography [7]. The technique can be used to modify the adsorption properties of gold substrates for the attachment of proteins. Because proteins adsorb preferentially on some materials and are repelled by others, specific materials such as alkanethiols can be transferred via microcontact printing onto gold in order to functionalize it for protein patterning. However, proteins can also be directly transferred by the elastomeric stamp. Untreated PDMS provides a hydrophobic surface very much like the polystyrene used for adsorption of proteins in immunoassays. The process for protein patterning is as follows. A PDMS stamp is covered with protein solution for inking. This creates a monolayer of protein on the stamp surface. The stamp is rinsed and dried, and the pattern is then transferred onto a substrate. Contact need only be made for a few seconds and pattern transfer occurs only where the stamp contacts the substrate. Immunoglobulin G (IgG) protein was transferred onto a silicon wafer using a stamp made of the siloxane Sylgard 184. Features with dimensions as small as 500 nm were replicated. Atomic force microscopy (AFM) imaging verified that patterns had high contrast and resolution because the stamp was mechanically stable and proteins did not diffuse significantly across the surface. The features also retained their biological activity after printing.

For proteins that may not survive adsorption processes at surfaces, additional steps may be taken to immobilize them onto a substrate although this lengthens and complicates the process [8]. Aside from proteins, other patterned materials include lipid bilayers and poly(amino acids). In the case of lipid bilayers however, the printed lines were expected to be 9-μm wide, but were actually 19-μm wide. Because PDMS is deformable it would not be surprising if areas surrounding the intended pattern also made contact with the substrate.

Microcontact printing is suitable for printing over large areas at once. However, resolution is limited by the feature size of the master, mechanical deformation of the stamp and ink diffusion around the contact areas. The resolution may be improved by using stamps of higher stiffness. However, high-resolution masters require electron-

beam patterning and reactive ion etching of a silicon-on-insulator (SOI) wafer. Michel et al. [9] used a high-stiffness PDMS stamp with 80-nm-diameter posts to transfer single antibody molecules. Although they claim 99% transfer efficiency, the resulting spots were not regular in size and shape. Finally, a major feature of microcontact printing is that the flexible silicone stamps require a casting mold, the master, with a predefined layout. This may be costly and may necessitate a series of photolithography processing steps [10].

5.2.2 Optical Lithography

The photolithographic technique can create DNA patterns with feature sizes as small as 18 μm [5]; however, it is expensive and places a limit on the allowable oligonucleotide length. For reliable detection of each gene, ten to 20 probes are needed, thereby limiting arrays to about 12000 genes per square centimeter. Smaller feature sizes are possible using polymeric photoresists used in the semiconductor industry which exhibit a nonlinear response to illumination intensity. Features as small as 8 μm have been constructed in this manner. UV lithography can be used to directly pattern alkanethiol SAMs with micron-scale resolution [11]. It is then possible to attach biomolecules to these patterns.

Lithographic patterning of DNA operates as follows (Fig. 5.1). Synthetic linkers modified with photochemically removable protecting groups are attached to a glass substrate [12]. The substrate is exposed to light directed through a mask to selectively deprotect and activate certain sites. Protected nucleotides can then attach to these

Table 5.1. Techniques suitable for use in the life sciences

Deposition method	Best resolution	Ink	Substrate	Reference
Microcontact printing	500 nm	IgG protein		[7]
	19 μm	Lipid bilayers		[8]
Optical lithography	8 μm	Alkanethiols		[11]
	500 nm	Streptavidin		[16]
Dip-pen nanolithography	30-nm lines	Collagen	Gold	[43]
	45-nm dots	IgG protein		[44]
Surface patterning tool	2–3-μm dots	Cy3-streptavidin		[51]
	150-nm lines	Quantum dots conjugated to streptavidin		
Microspotters	30-μm dots	IgG protein and oligonucleotides	Glass	[53]
Nanopipettes	440-nm dots	IgG protein	Glass	[61]
	510-nm dots	Biotinylated DNA		
Nanofountain probe	40-nm lines	MHA	Gold	[35]
	200–300-nm dots	DNA		[67]
	200–300-nm dots	IgG protein		Unpublished

IgG immunoglobulin G, *MHA* 16-mercaptohexadecanoic acid

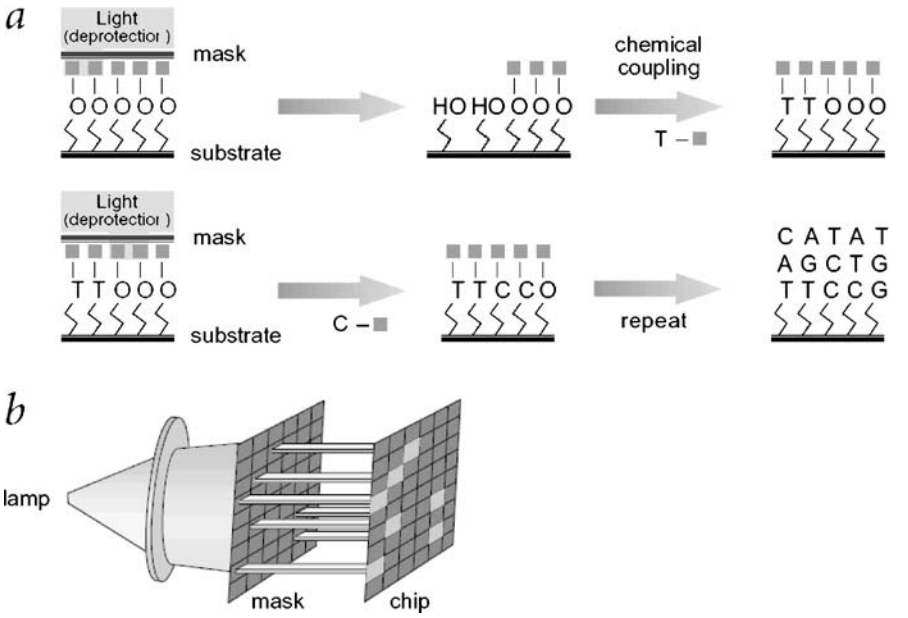

Fig. 5.1. a Photolithographic oligonucleotide synthesis. Light directed through a mask activates certain sites and protected nucleotides then couple to these sites. The process is repeated, with different sites being activated and different bases being coupled. **b** A lamp, mask and array [12]

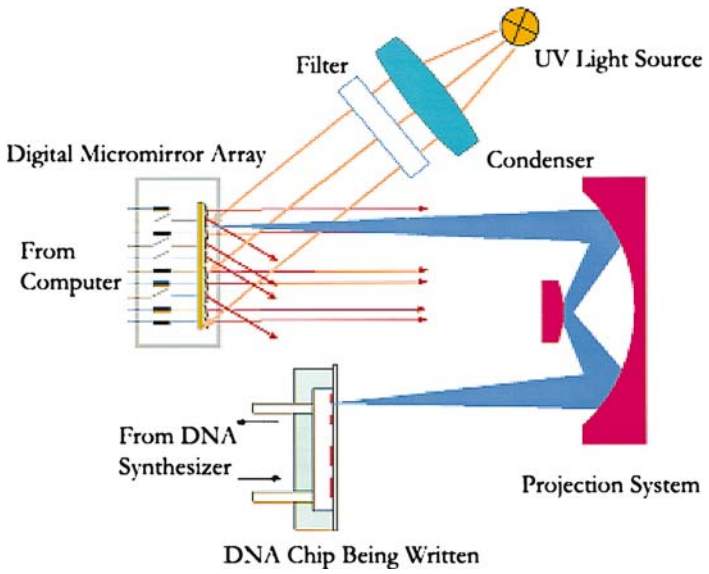

Fig. 5.2. The maskless array synthesizer [13]

sites. The process is repeated; coupling different bases allows arbitrary DNA probes to be constructed at each site. A drawback is that a changing set of monitored genes requires a new design and new masks. To overcome this, a maskless array synthesizer (MAS; Fig. 5.2) was developed [13]. Computer-generated virtual masks were relayed to a digital micromirror array which used 1:1 imaging to address pixels in a 10 mm × 14 mm area. The MAS system was used to print checkerboard patterns of 16-μm features (the size of each micromirror).

5.2.3 Protein Arrays

Protein patterning is useful for miniaturizing biochemical tests for high-throughput screening of new drug candidates and for performing studies in protein expression, protein–protein and protein–enzyme interactions and cell adhesion. Whereas DNA microarrays have been well established for genomics, no such high-throughput technologies yet exist for proteomics [14]. However, advances are being made and there are many protein array suppliers for the wide range of applications for which they are needed. (Listings are found in [14, 15]). For the photolithographic production of submicron protein patterns, pH-responsive films were patterned by exposure to 365-nm light. This allowed for the conjugation of aminooxy-modified biotin and the subsequent immobilization of streptavidin. Protein patterns as small as 500 nm were produced [16].

A conventional assay technique is the enzyme-linked immunosorbent assay (ELISA; Fig. 5.3), used to detect peptides, proteins, antibodies or hormones [17, 18].

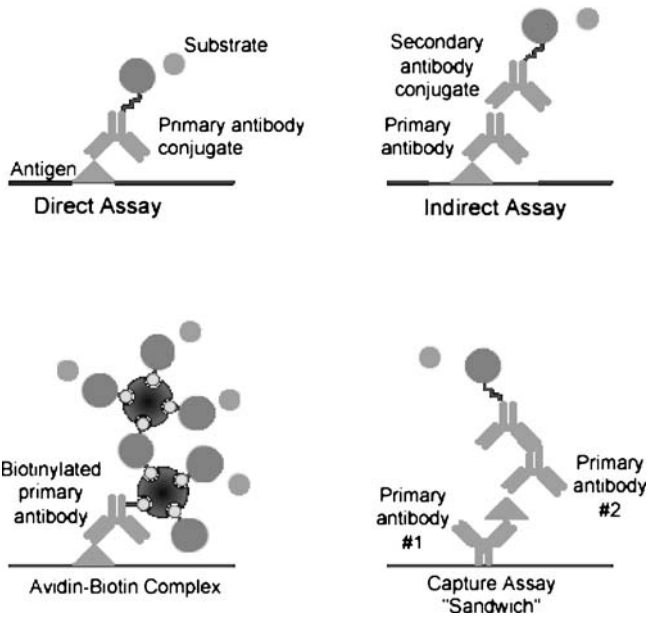

Fig. 5.3. ELISA immunoassay formats [17]

For antibody detection, an antigen is immobilized on a solid support. The sample for inquiry (any body fluid) is applied, and if the antibody in question is present it will bind to the antigen. Detection is accomplished via an enzyme directly linked to this primary antibody or a secondary antibody that recognizes the primary antibody. Or, if the primary antibody has been labeled with biotin, it can then be incubated with streptavidin. Incubation of this complex with an appropriate substrate produces a detectable product; typically a color change is imparted. The amount of color is measured proportional to the amount of antibody present in the sample. The most commonly used enzymes are horseradish peroxidase and alkaline phosphatase. ELISA is typically performed in 96-well or 384-well polystyrene plates coated with a ligand which will passively bind antibodies and protein; thus, unbound materials can be easily separated from the bound material during the assay. False positives are possible owing to the nonspecificity of protein–antibody interactions, and some analytes such as HIV require retesting using western blot, an electrophoretic technique where antibodies are directed against a number of viral proteins.

5.3 Nanoarray Technology

5.3.1 The Push for Nanoscale Detection

The delivery of biological material in increasingly smaller volumes has the potential to advance many applications. Studies of protein function are made possible, for instance, protein clustering in cell focal adhesion occurs at 5–200-nm length scales; delivery of material at this relevant length scale allows proteins of interest to be bound to a substrate [19]. Lateral control in creating specific adhesive and inert sites can create rigid ligand templates for cell binding. The specific interactions between binding pairs can be used for protein immobilization; these include affinity capture ligands (streptavidin–biotin binding) and antigen–antibody recognition for immunoassays [20]. Phospholipid deposition can be used to make model systems that can mimic the structural complexity of biological membranes [21]. It is also useful for studies investigating the binding of a protein and drug with supported lipid bilayers.

In the fabrication of arrays, it is important to reduce the sample volume, particularly in applications where limited sample amounts are available, such as in the analysis of multiple tumor markers from biopsy material [14]. Laser capture microdissection for cancer biomarker screening can obtain a few cells from a cancer tissue section, but it is very difficult to analyze the protein content of these cells using microarrays [22]. On the other hand, nanoarrays require only minute volumes of sample, approaching the volume of a single cell, so solid-phase testing on single cells can be performed.

A reduction in an array spot size suggests that statistically every molecule in an analyte has the opportunity to sample the entire capture surface in a reasonable amount of time [24]. In microarrays, not all of the sample will reach the capture surface unless energy is added to enhance the movement of the analyte, such as by agitation, mixing or electromotive force; thus, part of the analyte is effectively wasted.

Smaller arrays imply that biochemical reactions may not be diffusion-limited. In effect, nanoarrays offer the possibility of greater sensitivity in diagnostic tests, since disease progression is often correlated with protein levels [23]. Protein nanoarrays would be particularly useful, as protein signals cannot be amplified via methods such as polymerase chain reaction (PCR). Since many protein biomarkers are present in concentrations of only 10–100 pg/ml, improving assay sensitivity could lead to the discovery of new biomarkers that currently go undetected [24]. Essentially, the fabrication of nanoarrays will allow the screening of smaller volumes in shorter amounts of time. It will allow for higher-density arrays; one assay could then screen a greater number of targets.

Microarray analysis relies on optical readout methods, either by the observance of a color change as in ELISA, or the reading of fluoresence signals, which requires fluorescently labeled molecules for the detection of protein–protein interactions [25]. However, such labeling may cause deformational changes of the protein molecule, which may in turn affect the protein function. Radioisotopes are also sometimes used for labeling, but this requires the subsequent management of radioactive materials [26]. Labeling efficiency varies, so quantitation may not be reliable, and the labeling process is time-consuming and labor-intensive. For all these reasons, label-free detection is preferable. It also allows for real-time detection and in situ identification.

The atomic force microscope (Fig. 5.4) is an instrument capable of label-free sample analysis. It is a member of the family of scanning probe microscopes (SPM), which makes use of specialized probes to scan a sample surface to produce maps of topography, conductivity, binding force or friction among many others. These data sets can also be obtained all at once. The resolution of the technique is highly dependent on the probe quality and sharpness. Nanoarrays are well suited to atomic force microscope readout. For example, arrays for virus detection contain domains of

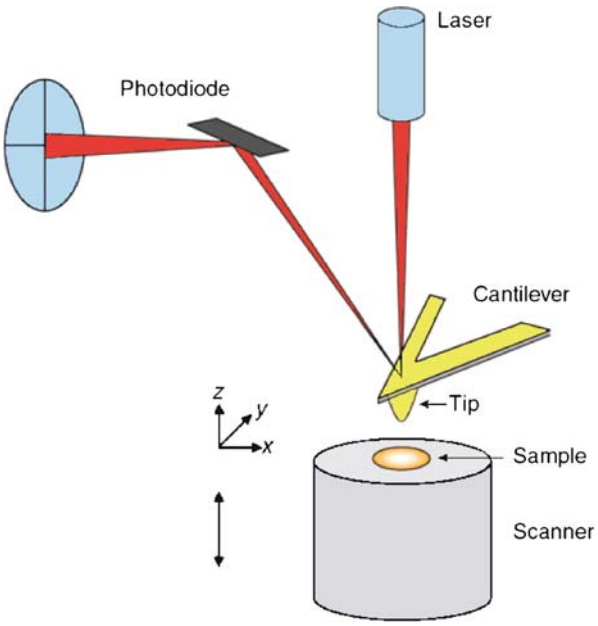

Fig. 5.4. Principle of atomic force microscopy (AFM). The sample is mounted on a piezoelectric scanner for three-dimensional positioning. The force between the tip and the surface is determined by measuring the cantilever deflection optically (with a laser and a photodiode) [28]

antibodies directed against specific viral species [22]. Any of these viruses present in a test solution will attach to certain domains and can be detected via AFM. A variety of solutions can be tested, including serum, sputum, sludge, coffee and urine, some of which inhibit other methods such as PCR. Perhaps most importantly, AFM is applicable in almost any environment, including liquids. This is required for studying cells and membranes in their native environment. Lastly, AFM-based methods are amenable to subsequent manipulation by the probe. For example, DNA can be induced to fold by controlled pushing by an atomic force microscope tip [27].

5.3.2 Probe-Based Patterning

The following section discusses a variety of scanning-probe-based lithography techniques suitable for use in the life sciences. They each have their own advantages and disadvantages. Their resolution and typical examples are given in Table 5.1. Many factors influence the ability to pattern very small features. These include environmental conditions, appropriate ink and substrate chemistry and the material and geometry of the probe tip.

5.3.2.1 Dip-Pen Nanolithography

Dip-pen nanolithography (DPN; Fig. 5.5) was first introduced to the research community in 1999 as a tool for patterning nanostructures, in which an atomic force microscope probe tip (approximately 20 nm radius) is dipped into a solution to coat it with the desired molecules [29, 30]. Patterning is typically accomplished with a commercial atomic force microscope which controls the movement of the probe. When the probe is brought into contact with a substrate, molecules diffuse from the probe to the substrate. In most cases, the ink molecules produce a local reactive functionalization of the surface, such that specific biochemical adhesion experiments can be conducted at these length scales. In general, the deposited material and the substrate must be paired, such that a chemical reaction occurs upon delivery, or a surface SAM is formed so that readout is possible using the atomic force microscope.

DPN is characterized by simplicity and high writing resolution (less than 100 nm). A large amount of literature is available on the use of single-probe DPN. Apertured probes [32, 33] can store and dispense larger numbers of ink molecules, but the writing speed is not increased substantially and the writing resolution is inferior to that of DPN. The resolution is affected by the geometry and aperture size of the probe tip and the wetting properties of the tip and the substrate. The smallest features produced were typically twice the diameter of the aperture; the smallest apertures produced were 35 nm in diameter [34]. Lastly, because such apertured probes are milled by a focused ion beam, they are not easily mass produced. Pulled-glass nanopipettes offer continuous ink delivery, but lower resolution (approximately 1 μm), and cannot be integrated by microfabrication into larger systems. Nanofountain probes (NFP) [35, 36] exhibit continuous ink delivery for a long-range writing capability, resolution close to that of DPN, and can be integrated in arrays and systems, although the probes and AFM systems become more complicated and costly.

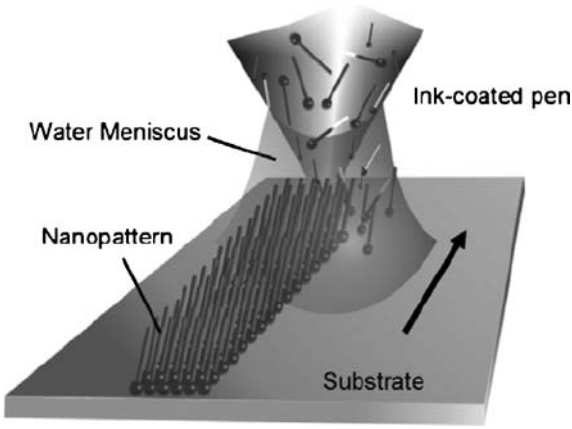

Fig. 5.5. Dip-pen nanolithography (DPN) patterning [31]

Indirect DPN

The most common demonstrations of DPN patterning have involved the deposition of *n*-alkanethiols onto gold surfaces because thiols self-assemble and strong thiol–gold bonds are formed [38]. The fabrication of patterns of biological materials began with indirect adsorption of the molecules of interest onto DPN-generated templates. 16-Mercaptohexadecanoic acid (MHA) could be deposited onto gold substrates via DPN; features as small as 100 nm were possible [39]. Nonpatterned areas were then passivated with 11-mercaptoundecyl tri(ethylene glycol) (PEG-SH). The desired proteins, lysozyme or rabbit IgG were attached by submersing the substrate into a 10 μg/ml protein solution for 1 h. No detectable nonspecific binding to the passivated areas was observed. It was also demonstrated that retronectin could adsorb specifically to the MHA-patterned dots 200 nm in diameter, spaced 700 nm apart. In turn, 3T3 Swiss fibroblast cells could be attached to these retronectin patterns, indicating that nanoarrays could be used for cell adhesion studies as well.

Metal ion-affinity templates can also be used to immobilize antibodies [40]. As metal ions are not susceptible to denaturation, they can be used as a linker to immobilize many unmodified polyclonal and monoclonal antibodies. First, DPN was used to pattern MHA spots. The surrounding areas were passivated with PEG-SH and the carboxylic acid groups of the MHA were coordinated to Zn^{II} ions. The substrates were then exposed to solutions of the desired antibody.

Indirect DPN techniques have the potential to be used for the creation of sandwich assays with the purpose of disease detection. For example, DPN can be used to deposit an array of MHA spots which then attract the p-24 antibody for HIV [41, 42]. The surrounding areas are passivated with bovine serum albumin. The array could then be used to detect HIV in patient samples, exceeding the detection limit of conventional ELISA-based immunoassays.

Direct DPN

Direct deposition of biological material eliminates the additional step of first patterning a linker molecule. It also eliminates cross-contamination of array features

because the desired chemistry is carried out only at specific locations [29]. This is essential for the prevention of nonspecific adsorption, which becomes an increasing problem as arrays get smaller—a few nonspecifically bound molecules may overwhelm the entire intended signal [26]. Silicon atomic force microscope tips were used to deposit thiolated native collagen (1 mg/ml in 1 mM HCl) and collagen-like peptides (40 mg/ml) onto gold substrates via DPN [43]. Line widths down to 30 nm were achieved. Collagen arrays could conceivably be used to induce an assembly network of collagen scaffoldings that would direct cell attachment or as guest–host systems for other biological entities.

In most cases, however, direct deposition by DPN typically requires prior chemical modification of the atomic force microscope tip. For example, commercial atomic force microscope tips functionalized with 0.1 mM thiotic acid could be used to deposit lysozyme and rabbit IgG (Fig. 5.6) [44]. The modified atomic force microscope tip was immersed in protein solution (500 μg/ml) for 1 h and then used to pattern immediately. The patterned IgG dots were 45–200 nm in diameter, and the biomolecules maintained their biorecognition properties after being patterned. The study demonstrated that multicomponent arrays could be patterned without cross-contamination. However, high humidity (80–90%) was required for successful patterning; a relative humidity below 70% resulted in inconsistent ink transport properties. Furthermore, the transport rate depended on the composition of the protein.

2-[Methoxypoly(ethyleneoxy)propyl]trimethoxysilane can also be used to functionalize atomic force microscope tips. The material forms a biocompatible and hydrophilic surface layer on the tip, and prevents protein adsorption and denaturation on the tip surface. It also reduces the activation energy for transporting proteins from the tip to the substrate. Without it, the protein solutions (500 μg/ml) do not wet the silicon nitride (Si_3N_4) cantilevers and inconsistent or low-density protein patterns are produced. Lim et al. [45] immersed such an atomic force microscope tip in protein solution for 1 min and used it to pattern in 60–90% relative humidity. Rabbit IgG features ranging from 55 to 550 nm were fabricated. It was also demonstrated that human, goat and mouse IgG, and anti-human, anti-goat and anti-mouse IgG could be patterned in this manner.

Nickel-coated Si_3N_4 atomic force microscope tips were used to deposit histidine-tagged ubiquitin (300 μg/ml) and thioredoxin (250 μg/ml) proteins onto nickel oxide surfaces [46]. As in the previous cases, bare Si_3N_4 cantilevers could not be coated homogeneously with the proteins, resulting in inconsistent or low-density protein patterns.

The proteins angiogenin and integrin $\alpha_v\beta_3$ were deposited using gold-coated silicon cantilevers functionalized for 30 min in 1 mM mercaptoundecanoic acid [25]. The resulting SAM increased tip hydrophilicity and facilitated protein adsorption on the tip surface. The tip was then immersed in the desired protein solution for 1 h and the molecules were patterned via DPN. The smallest spots created were 120-nm wide and protein transfer was found to be affected not only by the tip–substrate contact time but also by the contact force. In order to produce regular patterns, high humidity was required, as in the work in [44].

Demers et al. [47] used DPN to directly pattern hexanethiol-modified oligonucleotides on polycrystalline gold, and oligonucleotides bearing 59-terminal acrylamide groups on derivatized silica. The atomic force microscope tip had to be

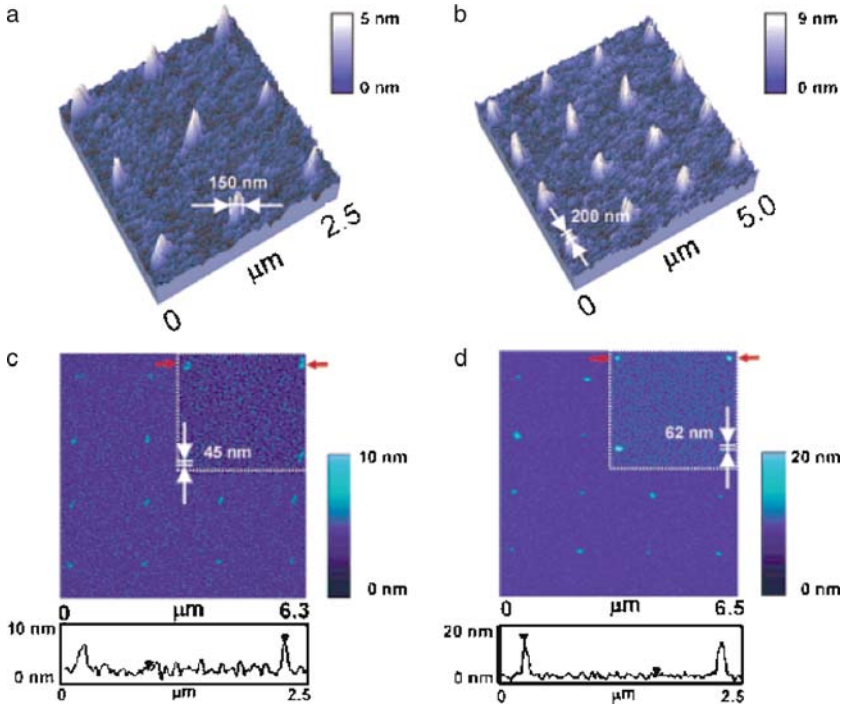

Fig. 5.6. AFM images of protein arrays generated via direct-write DPN. **a** Nanodot array of lysozyme; **b** array of immunoglobulin G (IgG); IgG dots before **c** and after **d** treatment with a solution of anti-IgG-coated nanoparticles [44]

first silanized by immersing it in a solution of 39-aminopropyltrimethoxysilane in toluene, to render it positively charged and hydrophilic.

Although protein delivery was not tested, PDMS-coated atomic force microscope tips were found to deliver MHA, octadecanethiol (ODT) and cystamine [48]. As cystamine is very volatile, its patterning via conventional DPN with Si_3N_4 tips is problematic. However, the PDMS-modified tips successfully patterned 200–300-nm-wide lines. The packing density of cystamine could be influenced by the writing speed. The PDMS acts as a reservoir that absorbs inks and allows for 1–2 h of continuous MHA patterning. The pattern resolution was not quite as good as that of regular DPN—the thinnest lines generated were 55-nm wide; however, these are much smaller features than can be obtained via methods such as microcontact printing.

It was demonstrated that a monolayer of succinic acid succinimidyl ester 5-thioyloxy-2-nitrobenzyl ester (SSTN) could be used as a photocleavable cross-linker to chemically link avidin to a gold-coated atomic force microscope tip [1]. When the tip was brought into contact with a biotinylated mica substrate, UV irradiation was applied to cleave the SSTN, releasing avidin onto the substrate. The protein-free atomic force microscope tip could then be used to image the deposited material. The delivered avidin was confined in a range of $100 \times 90\,\text{nm}^2$ and maintained its affinity to biotin.

Most DPN writing has been accomplished using the contact mode operation of the atomic force microscope. This is the most common method of AFM operation, in which the probe tip and the substrate remain in close contact while the substrate is being scanned. A drawback of this method is the exertion of large lateral forces on the substrate as the probe is dragged across it. In tapping mode AFM, a cantilever probe of lower stiffness is oscillated at its resonance frequency and taps the substrate for a small fraction of its oscillation period, thereby reducing the lateral force exerted on the substrate as well as the tip–substrate adhesion forces. Agarwal et al. [49] deposited a synthetic peptide MH_2 via tapping mode AFM, which allows for gentle imaging of deposited material as well as deposition on soft substrates. The drive amplitude was found to be a critical factor. When coated with peptide, the drive amplitude of the AFM probe decreased significantly, and as the peptide was being deposited, the drive amplitude required for imaging increased. In order to successfully deposit peptides in tapping mode, the drive amplitude had to be increased by a factor of 2–5 from its imaging value, causing the probe to exert a greater contact force on the substrate. Nevertheless this force is still less than that in contact mode DPN.

5.3.2.2 Open-Channel Pens

Reese et al. [5] micromachined stainless steel fountain pens (Fig. 5.7) with open trenches which narrowed to a width of 30 μm at the pen tip. The trench width dictated the patterned spot size; spots 10–30 μm wide and 20–140 μm long were deposited. The highest density arrays were 25,000 spots per square centimeter of fluorescent dye. With a single loading, a pen could print five to 20 spots. Printed oligonucleotides with a mean spot size around 3500 μm^2 were successfully hybridized. Nevertheless, such fountain pens are not capable of nanoscale patterning.

A device named the surface patterning tool (SPT) was developed by Henderson et al. [50]. An SPT consists of a cantilever with a split gap at the end, a reservoir on the handling chip, and a 1-μm-deep open transportation microchannel connecting the gap and the reservoir. Sample loading is carried out by filling the reservoir with sample solutions as well as by dipping the cantilever end into sample fluid. These designs, dedicated to biomolecular patterning, allowed reliable patterning of large molecular species and reduced reloading requirements. The length of the SPT cantilevers ranges between 200 and 300 μm, and the width ranges between 20 and 40 μm. The split gap is approximately 1 μm wide and approximately 40 μm long. At the fixed end of the cantilever, a 10-μm-deep rectangular reservoir is located on the handling substrate. The depth and the width of the microchannel are 1 μm and 1–10 μm, respectively.

Testing of the fabricated SPTs was performed using a dedicated commercial instrument called a NanoArrayer (BioForce Nanosciences, Ames, IA, USA). This instrument is equipped with a precision motion control system and an environmental chamber. Although this instrument uses the same optical lever deflection scheme employed in AFM, it does not scan or acquire images. SPTs are mounted to form a 12° angle with the deposition substrates such that only the tip end is in contact with the substrate. Patterning was demonstrated at a relative humidity of 35–50% using

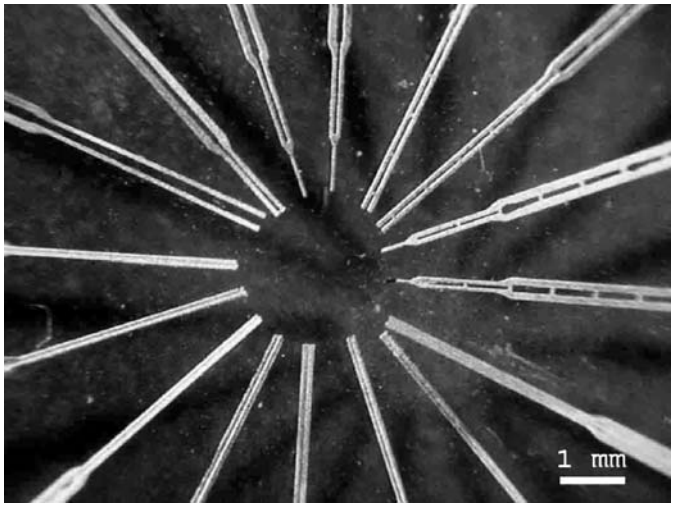

Fig. 5.7. Stainless steel fountain pens [5]

Cy3–streptavidin [50]. A 10 × 10 array of spots with a diameter of 2–3 μm was routinely obtained; this value was limited by the width of the SPT's split-gap. A single loading of the tool printed at least 3000 spots in about 1 h. It was also demonstrated that quantum dots conjugated to streptavidin could be deposited in patterns of lines and spots using the SPT. These features had line widths of approximately 150 nm to 7 μm and spot diameters of 3–5 μm [51].

5.3.2.3 Microspotters

In microspotting technologies, a biochemical sample is loaded into a spotting pin by capillary action, and a small volume is transferred to a solid surface by physical contact between the pin and the solid substrate [52]. Other than microspotting pins, capillaries or tweezers can act as a printhead of biochemical samples. Printheads can be moved by the *XYZ* motion control system of an atomic force microscope and brought into a contact with a surface to transfer the sample.

Belaubre et al. [53, 54] fabricated microspotters (Fig. 5.8) on SOI substrates using conventional micromachining techniques.

Arrays of 2-mm-long, 210-μm-wide and 5-μm-thick cantilevers, spaced 450 μm apart, were microfabricated. These cantilevers were used to pattern a glass slide with 1-pl volumes of a solution containing cyanine3-labeled oligonucleotides (15-mers) [53]. Anti-goat IgG (rabbit), microarrays were also generated on a glass slide coated with dendrimer molecules as cross-linkers. In both cases, 30-μm-diameter spots were obtained. It was also demonstrated that no cross-contamination was observed for two different biological samples deposited with the same cantilevers if a cleaning procedure was used. Using a similar microspotter, Leichle et al. [55] deposited colloidal solutions containing poly(ethylene glycol) 600 and aminopropy-

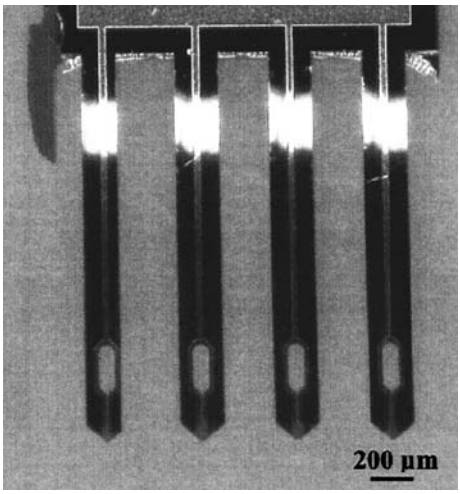

Fig. 5.8. Microspotter array [53]

ltriethoxysilane nanoparticles with diameters of approximately 300 and approximately 150 nm, respectively, on surfaces to form spots with diameters ranging from approximately 10 µm to more than 100 µm.

To further reduce droplet size, Saya et al. [56] introduced a technique to fabricate an in-plane sharp nanotip incorporated into the channel of a cantilever (Fig. 5.9). Tips with a curvature radius less than 100 nm were fabricated, and were connected to V-shaped microchannels 5 µm wide. The cantilevers were used to deliver water–glycerol droplets. The surface wettability of the nanotip and the substrate were important factors in determining the droplet size. For a hydrophilic tip contacting a hydrophobic substrate, droplets 3–4 µm in diameter were achieved, and the contact time did not significantly affect the drop size. Smaller droplets 2 µm in diameter could be achieved with high uniformity using a hydrophobic tip and a hydrophilic substrate; however, the contact force and time affected the spot size.

Pens with open microchannels integrated on cantilevers have the advantage of being clog-free and allow for easy cleaning and simple microfabrication. However, such open microfluidic elements such as microchannels and reservoirs are prone to cross-contamination via vapor from different types of samples, especially when loaded in arrays of cantilevers [57]. Evaporation may be critical in

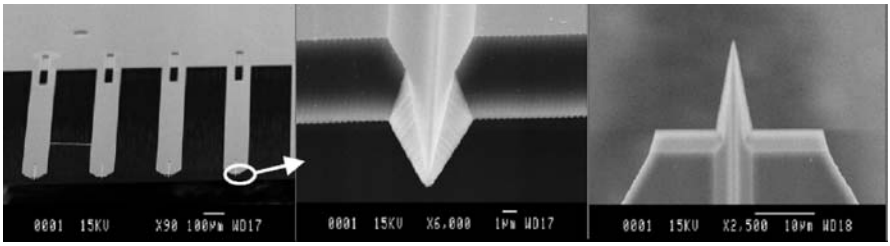

Fig. 5.9. Scanning electron microscopy (SEM) images of a cantilever array (*left*) with a nanotip (*center* and *right*) [56]

some applications although its rate can be reduced with environmental conditioning. Enclosed microchannels are beneficial in such cases, although they are more difficult to microfabricate and are subject to clogging. Pipettes are conventionally used microfluidic devices with enclosed channels. Microneedles with embedded microchannels were also demonstrated to deliver liquid materials [58]. In the following subsections, microcantilever devices with enclosed microchannels are described.

5.3.2.4 Pipettes

Bruckbauer et al. [59] developed a delivery system based on scanning ion-conductance microscopy. In this voltage-controlled nanopipette, an ion current flows between an electrode in the pipette and one in a bath; the pipette acts as the ink reservoir. Deposition of molecules to a surface occurs in the presence of aqueous buffer. Protein G was successfully delivered using the pipette. Biotin and single-standed DNA with spot sizes of 830–860 nm were also deposited.

Following this, goat anti-rabbit IgG antibody was delivered onto charged glass, with spot sizes of about 2 μm [60]. The flow of molecules began at an applied voltage of −0.5 V and increased linearly with applied voltage between −1.0 and −1.5 V. Although voltage control allows for the control of ink delivery at the single-molecule level, the diffusion of molecules in solution and on the substrate ultimately increases the patterned feature size. Because the nanopipette deposits in solution, protein denaturation may be prevented. However, the use of voltage subjects the sample to a high electric field. Nevertheless, owing to the small current, very little heating (less than 1 K) occurs. Indeed, the biomolecules were demonstrated to maintain their functionality after deposition. This was demonstrated via binding experiments with IgG and hybridization studies with DNA.

In order to reduce the patterned feature size, a double-barreled nanopipette (Fig. 5.10) operating in air was fabricated from 1.5-mm-diameter pulled-glass capillaries with a septum down the center [61]. The device was used to deliver fluorescently labeled rabbit IgG to a polyethyleneimine-coated glass surface, with the smallest spot produced being about 440 nm in diameter. Biotinylated DNA was delivered onto streptavidin-coated glass with an average spot size of 510 ± 40 nm for a 5-s deposition time. In both cases, molecules were delivered out of one barrel at any one time. Distinguishing itself from the original nanopipette, the double-barreled pipette could write with two different inks. Two different, noncomplementary sequences of biotinylated DNA were loaded into the barrels. The DNA to be patterned could be selected by changing the sign of the applied voltage. The two inks could be delivered to the same location on a substrate. The double-barreled pipette is also capable of topographical scanning but its resolution is not as good as that of AFM; it cannot track up steep slopes or tight grooves as effectively. Most recently, the double-barreled pipette was used to deposit water droplets, working under oil [62].

A major drawback of this device is that it is not easily scalable because the pipettes are individually fabricated by laser pulling. The smallest pipette that can be made using this approach has a radius of approximately 20 nm, limiting the pattern resolution [63].

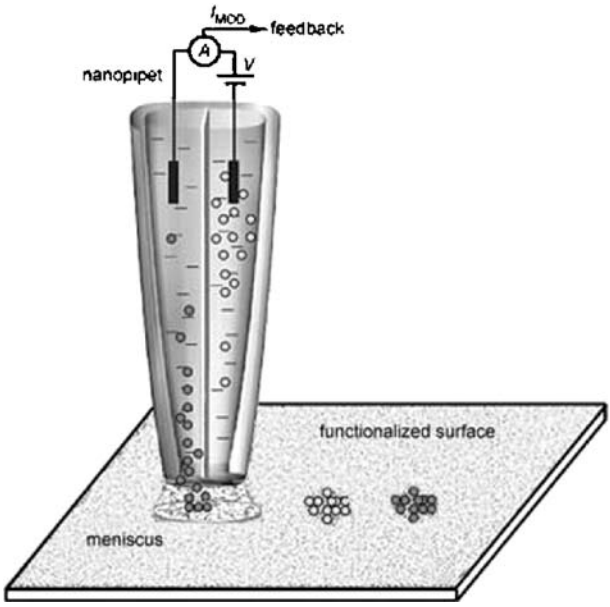

Fig. 5.10. Principle of double-barreled pipette deposition. The voltage between the two barrels controls the molecular delivery [61]

5.3.2.5 Closed-Channel Cantilevers

The concept of the nanofountain probe (NFP) was first introduced by Espinosa and coworkers in [64–66]. The device allows for both high-resolution patterning and continuous sample feeding through closed microchannels. The chip without its cantilevers has an overall size of 1.8 mm × 3.2 mm to fit easily into commercial AFM equipment. In the latest version of this chip, the two opposing sides of the chip each have 12 cantilevers; one set is 520 μm long and the other is 430 μm long. A volcano-like dispensing tip (Fig. 5.11) exists at the end of each cantilever and has a ring-shaped aperture and is able to generate sub-100-nm lines routinely.

For fast-evaporating solutions such as alkanethiols, the writing mode is similar to that of DPN, and pattern resolution is controlled by the radius of the core tip, not the aperture size. MHA (1 mM) in ethanol with line widths as small as 40 nm was patterned onto a gold substrate at a humidity of 60% using the NFP [35]. The NFP's imaging capability in topography was similar to results obtained using commercially available atomic force microscope tips, and its sensitivity in lateral-force imaging was better than with commercial tips, an advantage when imaging SAM patterns. This imaging capability is essential for immediate examination of deposited patterns and also serves as a means for realigning probes when writing multiple materials.

In typical operation, however, the NFP preserves the liquid state of the ink during the patterning process [36]. The liquid present near the writing tip provides a continuous source of solvent vapor, preserving a high local solvent vapor pressure, which may contribute to the formation of a more vigorous capillary condensation meniscus [65]. Solvent vapors may also condense on the substrate, leading to a solvent

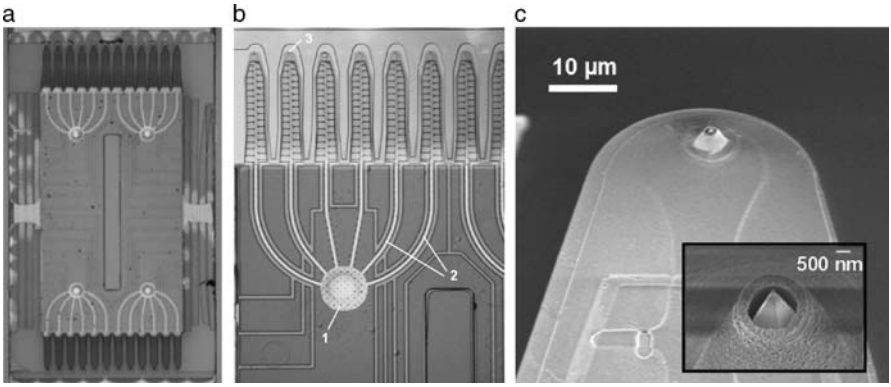

Fig. 5.11. Second-generation nanofountain probe (NFP) chip. **a** Optical image of the front view of an NFP chip **b** Closeup view of the chip showing *1* on-chip reservoir, *2* microchannels and *3* volcano tip **c** SEM image of a cantilever integrated with a volcano-like tip at the end; *inset* closeup of the volcano tip [36]

prewetting layer in the vicinity of the tip. The transport of ink molecules may also occur by coevaporation with the solvent and recondensation. This mechanism may lead to feature-growth dynamics different from that of DPN.

Batch fabrication allows for straightforward scaling to NFP arrays. Indeed, 12-cantilever NFP arrays have been fabricated, and their multiple on-chip reservoirs allow simultaneous patterning of two different solutions. Because the NFP can make use of two different reservoirs, it does not require a second tip to deposit an additional species. Simultaneous patterning with two different thiolate solutions, MHA and $1H,1H,2H,2H$-perfluorododecane-1-thiol in acetonitrile was demonstrated with the NFP [36]. Also, use of the NFP does not require repeated reinking and realignment of the tip during patterning, the latter of which is time-consuming and difficult to accomplish precisely. Finally, deep channels (more than 500 nm) allow the delivery of larger particles, including nanoparticles [37]. High compliance of the core tip relative to the volcano shell structure was observed in the induced deformation during scanning electron microscopy (SEM) observation of dry tips and is helpful in preventing clogging of the probe orifice and mechanically aids the transfer of larger species from the volcano cavity to the substrate. However, this may negatively affect alignment accuracy.

What sets the NFP apart from other devices is that while nanopipettes, apertured pyramidal tips and quill-type SPTs function by the formation of an outer meniscus between the probe and the substrate, the NFP forms a meniscus between the ultra-sharp atomic force microscope-like tip and the substrate, as in DPN. However, the NFP does not require modification of the tip surface in order to deliver biomolecules, because solutions are directly delivered from the on-chip reservoir to the tip. The NFP was capable of *direct* deposition of hexanethiol-modified oligonucleotides on a gold substrate [58, 67].

As shown in Fig. 5.12, the NFP was used to pattern a gold substrate with alkanethiol-modified oligonucleotides. After passivation of the unpatterned areas, the DNA spots were hybridized with complementary DNA-functionalized gold

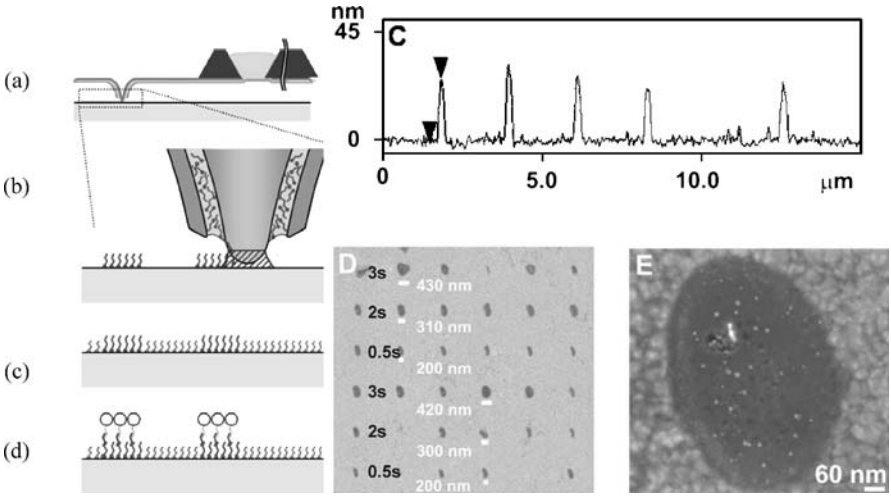

Fig. 5.12. Experimental procedure for DNA patterning: **a** molecular ink feeding, **b** direct patterning of a gold surface with alkanethiol-modified oligonucleotides, **c** passivation of the unpatterned areas with C6 thiol to avoid unspecific binding, **d** hybridization of the linker and probe DNA strands. **C** Height profile of the same array, acquired in tapping mode operation. **D**, **E** SEM image of a dot array and a single dot, respectively. Multiple gold nanoparticles are visible in **E** [67]

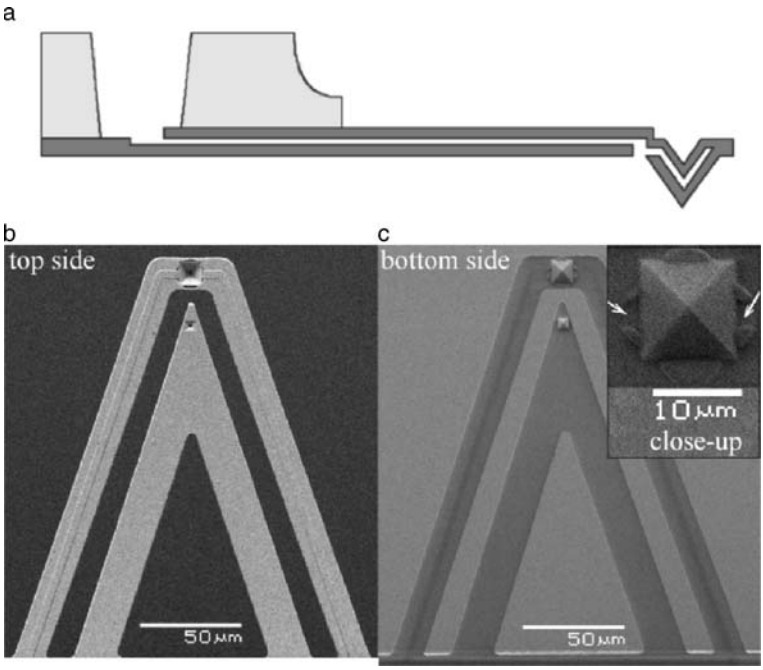

Fig. 5.13. a Cross section of the micromachined fountain pen; **b** *top view* and **c** *bottom view* of the fountain pen; *inset* closeup view of the pen tip, with outlet holes indicated by *arrows* [68]

nanoparticles (approximately 15 nm in diameter), demonstrating that the patterned DNA maintained its biological activity. Features 200–300 nm in diameter were routinely achieved.

A variation of the NFP concept introduced by Espinosa and coworkers [64, 65] was implemented by Deladi et al. [68,69] in a fountain pen consisting of two V-shaped cantilevers, one that is "multifunctional," and the other an inner cantilever solely for detection. A channel embedded in the first cantilever connected the reservoir to the tip. Two variations of this design were fabricated. In the first design, the outlet hole was located at the apex of the pyramidal probe tip, and had to be fabricated by focused ion beam milling, a process which must be done individually on each pen. The second design made use of batch processing, which dictated an opening at the base of the pyramid (Fig. 5.13). The pen allowed for continuous fluid supply. It was demonstrated that etchant could be delivered to etch chromium; the thinnest line etched was 350 nm wide and 14 nm deep. The thinnest features constructed were 500-nm-thick ODT lines on gold substrates.

5.3.3 Alternative Patterning Methods

5.3.3.1 Nanografting

Nanografting is a technique similar to DPN, but involves material removal as well as deposition. The basic procedure involves scanning a SAM on a substrate with an atomic force microscope tip using a force greater than the threshold force needed to displace SAM molecules [70]. SAM molecules are thus removed, and thiol inks previously adsorbed on the atomic force microscope tip can be adsorbed to these areas of the substrate. Care must be taken not to cause plastic deformation of the substrate beneath the SAM. Xu et al. [70] nanografted thiol solutions with concentrations ranging from 2 μM to 2 mM; the concentration did not appear to be a critical parameter in grafting. On the other hand, the scan rate was important. Slow scans often resulted in distorted patterns due to thermal drifts, but fast scans did not produce patterns with sufficient coverage. Liu et al. [71] demonstrated that alkanethiol features as small as $2 \times 4\ \text{nm}^2$, and 10-nm-wide lines could be produced via nanografting. Wadu-Mesthrige et al. [2] used nanografting to prepattern SAMs with thiols terminated with protein-adhesive groups such as aldehyde and carboxylate, which would then dictate the subsequent adsorption of proteins. Nanopatterns of lysozyme, bovine serum albumin and rabbit IgG were fabricated, with lateral dimensions ranging from 10 nm to 1 μm.

5.3.3.2 Conductive DPN

In AFM charge writing, positive or negative surface charge patterns are created on an insulating substrate such as a polymer or silicon dioxide by applying voltage to an atomic force microscope tip. Mesquida et al. [10] created microarray charge patterns on poly(methyl methacrylate) substrates which were then immersed in

water-in-perfluorinated oil emulsions where the water microdroplets were filled with $TTR_{105–115}$ peptide fibrils. The fibrils then attached to the charge patterns. The resolution was mainly limited by the size of the water droplets, which can typically be up to 5 μm in diameter. The use of water droplets as "containers" is advantageous in that the attachment process depends little on the content of the droplets, allowing the patterning of a variety of nano-sized biological materials.

Naujoks and Stemmer [72] used the same method to attach IgG–biotin stabilized emulsion droplets onto positively charged patterns. After drying, the protein molecules and salt from the buffer solution were left behind. The resulting spot sizes varied from 0.5 to 1.5 μm (Fig. 5.14). For these experiments, an atomic force microscope was operated in Kelvin probe force microscopy mode, where the lateral resolution was known to be in the range 50–100 nm, defined by the long range of electric forces and the geometry of the atomic force microscope tip. The pattern resolution might be enhanced by finding optimal emulsifying parameters and process conditions such as immersion time and drying ambiance.

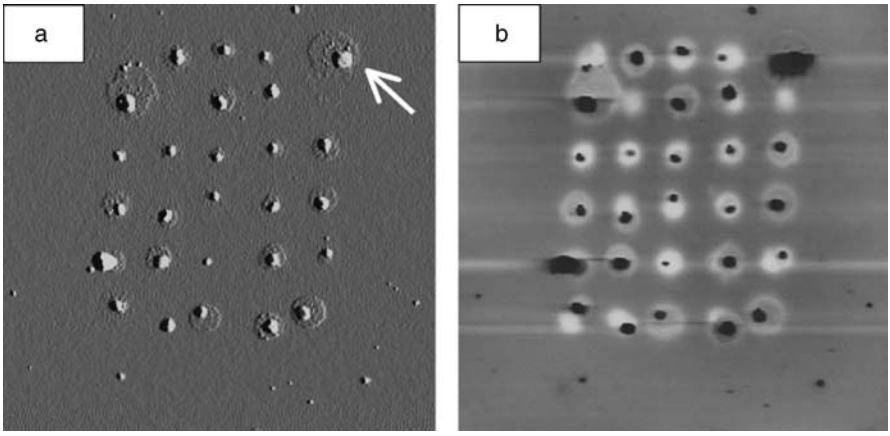

Fig. 5.14. a AFM (topography) image of IgG–biotin deposited on poly(methyl methacrylate). **b** Kelvin probe force microscopy (surface potential) image of positive charge pattern [72]

5.3.3.3 Electrochemical DPN

For the direct patterning of biological material, Agarwal et al. [73] used electrochemical DPN (e-DPN) to deposit a histidine-tagged peptide MH_2 and the histidine-tagged protein TlpA in tapping mode. An ionized nickel-coated substrate was held at ground potential and a negative bias was applied to the AFM probe tip. The method takes advantage of nickel–histidine binding and requires that a potential of about −2 V be applied. No functionalization of the silicon AFM probes was necessary. They were simply coated by immersing them in the desired solution for 15–30 s and then air-dried before patterning.

5.4 Nanoscale Deposition Mechanisms

Reproducibility is a concern for any fabrication technique. Nanopatterning results are not always repeatable and the resulting features are not necessarily well formed. An understanding of the ink deposition process is essential; however, in DPN, the mechanism for ink transfer is not completely understood and there is much controversy. It has been generally accepted that DPN patterning involves two processes: first, the transport of the molecular species from the atomic force microscope tip to the substrate through a water meniscus and, second, the adsorption of the ink onto the substrate. Control of these processes then would ultimately control the patterned feature resolution. Most studies on the patterning mechanism thus far have focused on the deposition of alkanethiols.

Theoretical studies on the dynamics of self-assembly have been performed in order to investigate the effects of deposition and atomic force microscope tip scanning rates on the resulting patterns generated via DPN [74]. The DPN process was treated as a two-dimensional Fickian diffusion process with a fixed source. Ink molecules on the atomic force microscope tip were driven by a concentration gradient to be deposited on a substrate. They then diffused over a monolayer of existing ink, and the diffusion was terminated by binding of the molecules to the bare substrate. In the patterning of dots by holding an atomic force microscope tip in contact with a substrate, the constant flux model predicted a $t^{1/2}$ dependence of the dot diameter, where t is the tip–substrate contact time. For the same number of molecules deposited, the final spot radius converged to the same value at long times, independent of the deposition rate. Increasing the diffusivity over the bare substrate resulted in circles that were fuzzier and not as well defined. For the generation of more complex patterns such as lines, a moving tip was needed and the tip scan rate had to be considered. In general, a fast scan or a slow deposition rate enhanced resolution, but as the scan rate increased further, patterned lines were no longer continuous. Such studies underline the necessity of determining optimal scan and deposition rates in order to produce coherent patterns using DPN. However, the effects of temperature, relative humidity and the presence of a water meniscus were not accounted for in these studies.

It is known that in ambient conditions, a water meniscus exists between an atomic force microscope tip and a substrate, and its volume increases with increasing relative humidity [75]. There have been suggestions that ink molecule transport occurs through this meniscus; however, Sheehan and Whitman [75] found that facile ODT deposition occurred even at 0% relative humidity in dry nitrogen. Since ODT is water-insoluble, its transport is not easily explained using a water meniscus model.

Cho et al. [76] proposed a “double-molecular layer” model in which the molecular ink on the atomic force microscope tip consists of a bulk solid region covered by a thin mobile layer on the surface (Fig. 5.15). A melting transition is suggested to explain the observed temperature dependence of the growth rate of patterns. The solid region serves as a reservoir of ink molecules which regulates the density of the surface layer, and the mobility and the number density of the mobile layer determine the molecular transport rate in DPN. It was proposed that three properties affect the mobility of the surface molecules—thermal energy, which increases the diffusion constant, residual solvent, which enhances diffusion of surface molecules, and ad-

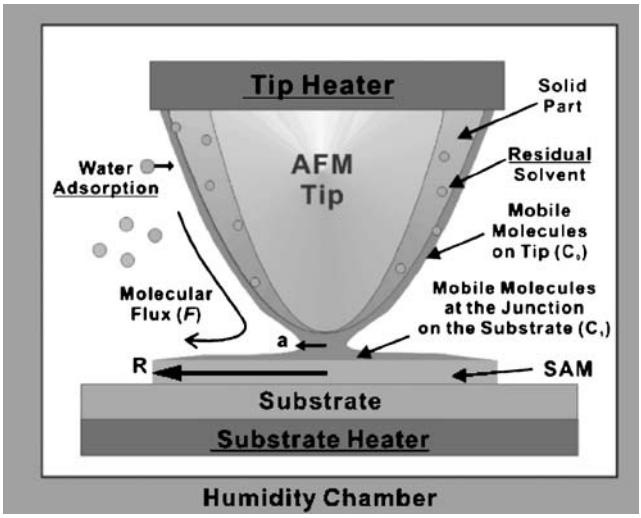

Fig. 5.15. Double molecular layer model for molecular ink transport [76]. *SAM* self-assembled monolayer

sorbed water, which enhances the mobility of hydrophilic molecular inks such as MHA and biomolecules.

In the general case where the diffusion and deposition rates are on the same order,

$$R \propto t^{\upsilon} \quad \text{and} \quad 1/3 \leq \nu \leq 1/2 \,,$$

where R is the radius of a patterned dot, t is the tip–substrate contact time and ν is the scaling parameter. ν approaches $1/3$ as the deposition rate becomes comparable to the diffusion rate, and $\nu = 1/2$ in a constant deposition case. In the patterning of ODT, a hydrophobic ink, on gold substrates, there are unstable fluctuations in the scaling parameter. These experimental results were explained using the double-molecular layer model. Above the melting temperature of ODT, the solid region melts and a single molecular layer forms. There is no longer a solid "reservoir" that regulates the density of the surface layer, leading to the unstable fluctuations in ν. Essentially there is a phase transition of the molecular species moving through the nanoscale junction. In the patterning of MHA, the scaling parameter increases with increasing relative humidity. It is suggested that adsorbed water enhances the diffusion constant on the substrate more than it enhances the transport rate at the tip–substrate contact point, implying that water molecules are also adsorbed on the SAM regions, not just on the probe tip.

In any case, direct environmental SEM (ESEM) observations verified that the height of the water meniscus between a silicon nitride probe tip and a gold or silicon substrate increases exponentially with increasing relative humidity [77]. In addition, for gold substrates, there was no observable meniscus below a relative humidity of about 70%, although, since the ESEM resolution in the imaging conditions used was approximately 50 nm, it is possible there was still a small meniscus. Still, these

results are consistent with experimental results for the patterning of MHA, in which there was little increase in the patterning rate at relative humidity between 0 and 50%, while the rate increased significantly at a relative humidity above 50%.

AFM studies by Rozhok et al. [78] of water meniscus formation between a probe tip and a NaCl substrate suggested that even at 0% relative humidity as defined by Sheehan and Whitman, water on the substrate will collect at the point of contact form to a meniscus. As it is very difficult to remove adlayers of water from surfaces, a small meniscus will typically form, even when a hydrophobic atomic force microscope tip is used. Only in ultra-high-vacuum conditions can the meniscus be eliminated.

Weeks et al. [79] found no observable MHA deposition at a relative humidity below 15%. This was attributed to the lack of meniscus formation. Increasing the humidity increased the patterned dot size for a given tip–substrate contact time. The group proposed that the DPN deposition process transitions from a dissolution-dominated regime to a diffusion-dominated one. For the fabrication of small alkanethiol features, the most important parameter is the activation energy of thiol detachment from the atomic force microscope tip. This transition occurs at a particular contact time, independent of the relative humidity. For short contact times, the transfer process is dominated by surface kinetics, whereas for long contact times, it is controlled by diffusion. Furthermore, no effect of contact force was observed; the water meniscus causes a capillary force between the tip and the substrate that is much greater, so capillarity dominates the total load force. This is in agreement with Zou et al. [80], who concluded that feature size is independent of contact force over a range from 0 to 10 nN.

It is thus fairly well agreed upon that the molecule transport rate is different in the fabrication of small and large patterns. It is slower for large features (longer tip dwell times) because the cantilever continues to deposit molecules on an area that has already been patterned. Ink depletion on the surface of the atomic force microscope tip also contributes to this phenomenon. Moreover, there is an equilibration time when patterning begins. This may imply that the solvent plays an important role in determining the mobility of the ink on the cantilever [81]. It may also be due to the fact that a water meniscus takes time to reach an equilibrium width when patterning begins, as observed via ESEM [82]. Moreover, the transport of thiol inks is affected by the state of the substrate, not only the ink already present on the substrate, but also adsorbates that may unintentionally be present. Uncontrolled surface chemistry may be one factor leading to differing results found in the DPN literature.

Schwartz [83] contends that the water meniscus is not universally responsible for molecular transport in DPN. In contrast to many other experimental results, both ODT and MHA were readily patterned on a gold substrate at 0.0% relative humidity. Two different but compatible models were proposed. For less polar molecules such as ODT, molecular transport occurs via molecular surface diffusion, known as “reactive spreading” in microcontact printing. This process depends on thermal energy. The second model is relevant to the transport of small ions such as DNA, as a solution in adsorbed water, and is compatible with the humidity dependence of the patterning rate of certain molecules. The degree of polarity of a molecule will determine its patterning behavior between the two extreme models. It has been suggested that MHA transport is due to two mechanisms. At low to moderate (50%) relative humidity, transport is caused by thermally activated surface diffusion [84]. As hu-

midity is increased, dissolution and bulk transport enhance the transport rate; above 70% humidity, the water meniscus begins to have an effect as well. Furthermore, surface water is not responsible for molecular transport.

This is consistent with MHA dot patterns generated at high humidity [85]. At relative humidity less than 80%, filled MHA dot patterns were always observed, but increasing the humidity to approximately 84% resulted in the formation of hollow ring structures. A bulk meniscus transport model cannot explain such patterns because it predicts only filled circles. Rather, an annular diffusion model proposed that ink molecules are transported at the air–interface of the meniscus.

Whereas the models mentioned previously could describe the deposition of molecules which bind strongly to their substrates, Manandhar et al. [86] investigated the anomalous patterns formed by the weak binding of 1-dodecylamine (DDA) on mica, which cannot be explained by random walks. Anomalous patterns are sometimes formed when surface binding is weak and interactions between molecules dominates, determining the final pattern. For DDA, small patterns are isotropic, but become more anisotropic as the pattern size increases. Thus, to create large, regular patterns it may be necessary to move the atomic force microscope tip to fill the area, instead of relying on diffusion to produce the final pattern. Finally, a constant deposition rate was observed, implying that stable DPN writing is possible even for weak-binding cases. Lee and Hong [87] developed a theoretical model to explain these irregular patterns. The corresponding computer simulations showed that in the presence of strong intermolecular interactions and preferential substrate–molecule interactions while the diffusive motion of individual molecules is suppressed, irregular star patterns and fractal-like structures can be formed. On the other hand, if the intermolecular interactions between deposited molecules are weak relative to the thermal energy, diffusive motion becomes important and regular circular patterns are formed as predicted by random-walk models.

Beyond the physical capability of patterning dots with specific sizes, there is the question of the appropriate feature size for a particular application. In biodetection, there exists an optimal spot size for the attainment of a robust diagnostic readout. Individual molecules are dynamic in nature; in order to obtain a good signal there must be many sampling events or long sampling times for a single molecule. Array spots smaller than a certain size will not have enough active and correctly oriented capture molecules, leading to inaccurate quantitation and reduced dynamic range [24]. It was estimated that for typical IgG, the number of molecules in a 1-μm-diameter spot is on the order of 10^4 whereas a 250-nm-diameter spot will have on the order of 10^3 molecules. Spots below this 250-nm threshold may lack a sufficient number of molecules for reliable quantitative data to be obtained. Further studies must be conducted to determine the optimal feature size for particular bioassays.

5.5 AFM Parallelization

One requirement for a deposition technique is its capability for high-throughput patterning. A particular device design should be scalable, i.e., its ink-delivery probe should be arrayable and it should be possible to fabricate the entire device in mass quantities.

5.5.1 One-Dimensional Arrays

Xu et al. [88] reported a second version of the quill-type SPT described in Sect. 5.3.2.2, in which five cantilevers were arranged linearly (Fig. 5.16) [88]. The microcantilevers and corresponding microfluidic network were capable of transporting multiple fluid samples from macroscale reservoirs located on the SPT substrate through microscale channels to the distal end of the cantilevers. Five cantilevers and five reservoirs were arranged in a chip so that multiple biological samples could be transferred from the reservoirs to the SPT cantilever array. The overall size of an SPT chip was 3 mm × 6 mm. Each cantilever was 250 μm long, 30 μm wide and 2 μm thick, while consecutive cantilevers were separated by a spacing of 50 μm. The microchannel on each cantilever was 15 μm wide and 1 μm deep. Multiple ink loading and patterning were tested using two different fluorescent protein solutions, Cy2–donkey anti-goat IgG and Texas Red–donkey anti-rabbit IgG in phosphate-buffered saline, and alternatively loaded into the five reservoirs by hand-pipetting. The solutions transferred from the reservoirs to the distal end of each channel by capillary action and the fluids were confined inside the microchannels without observed cross-contamination. A dithiobis(succinimidyl undecanoate)/gold surface was patterned to generate 10 × 10 multiple-ink dot arrays, with the mean spot diameter being about 12 μm. The SPTs generated biological arrays with a routine spot size of 2–3 μm. Several thousand spots could be printed without reloading. The minimum spot size of the SPT was mainly limited by its gap width, which could be further reduced with a higher-resolution lithography technique.

Using single AFM probes in DPN limits a pattern to the 90 μm × 90 μm scan size of the AFM instrument. In order to create patterns that span macroscopic distances on the order of centimeters, it is necessary to use multiple-pen cantilever arrays. A 26-pen array of cantilevers was used to pattern a 10 mM $NHSC_{11}SH$ acetonitrile solution

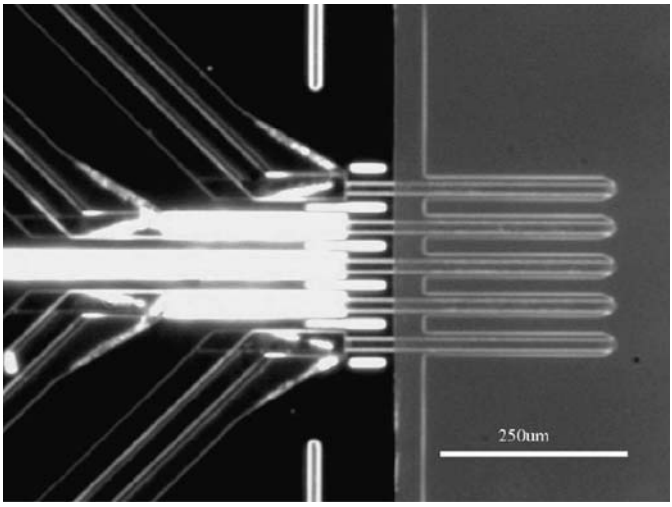

Fig. 5.16. Surface patterning tool cantilever array [88]

($NHSC_{11}SH$ is an amine-reactive alkyl thiol molecule) [89]. The surrounding areas on the substrate were passivated with PEG–SH. The dot array was then used as a template to immobilize protein A/G through covalent coupling. Highly dense arrays of 23,400 dots spaced 1 μm apart could be generated in this manner. The protein A/G templates could then be used for adsorption of human IgG, anti-β-galactosidase and anti-ubiquitin. It was demonstrated that the anti-β-galactosidase and anti-ubiquitin retained their biological activity after being deposited.

The second and third generations of the NFP introduced by Espinosa and coworkers allowed for multi-ink patterning using a linear array of 12 cantilevers [36, 66]. The device successfully deposited alkanethiols and oligonucelotides as described in Sect. 5.3.2.5, as well as bovine serum albumin and IgG proteins and gold nanoparticles [37].

5.5.2 Two-Dimensional Arrays

The IBM Millipede was likely the first example of a massively parallel cantilever array. The chip was an array of 32×32 cantilevers conceived for data storage using polymer thermal indentation [90, 91]. Feedback control in the z direction brought the entire array into contact with a substrate. This simplified the system but imposed a strict requirement on the uniformity of tip height and cantilever bending in order to minimize tip wear due to force variations over the array. Another two-dimensional cantilever array includes a 25×40 array of nickel probes fabricated by Zou et al. [80], with a tip-to-tip distance of 100 μm in the x and y directions.

In an initial attempt at a very large scale array for DPN, a 55,000-pen two-dimensional array occupying 1 cm^2 was fabricated using lithographic techniques [92]. The pens were spaced 90 and 20 μm apart in the x and y directions, respectively. As is the case for all arrays, the tips must all be aligned prior to patterning. Rather than implementing feedback for each individual cantilever, a gravity-driven alignment method was used for this large array. Complex patterns of 80-nm ODT dots on a gold substrate were successfully generated. One challenge that remains with DPN arrays is the difficulty in realigning the array after reinking or switching inks. Another is the variability in the inking process. In most cases, when the DPN tip is inked, excess ink is removed by a high-pressure blast of air. In an effort to increase reproducibility in inking the tip, Rosner et al. [31] developed arrays of microfabricated inkwells to supply ink to specific cantilevers in a probe array. A noninked probe could then be used for pattern inspection. A slower scan speed could be used to obtain better image quality while minimizing contamination onto the pattern. The inkwells employ open-channel meniscus-driven flow in microchannels to bring fluid stored in 1-mm-diameter reservoirs to a series of appropriately spaced inkwells. Different inks can be loaded onto different tips on the same cantilever array, allowing for multicomponent patterning.

The 55,000-pen array was used to deposit 1,2-dioleoyl-*sn*-glycero-3-phosphocholine (DOPC), a phospholipid, via DPN onto substrates of silicon wafers, glass slides and evaporated metal films [21]. Line features as thin as approximately 93 nm were patterned. The probe tips were coated with ink by immersing them into inkwells for at least 30 min. It was observed that in ambient humidity (30–50%), the DOPC

did not flow onto the tips, but at a humidity greater than 70% the phospholipid ink became sufficiently fluid to easily coat the tips.

Although most cantilever probe arrays used in the experiments described are made of inorganic materials such as silicon, silicon nitride or other metals, polymer probes may be of interest because they offer different biochemical properties [80]. Furthermore, they have a smaller Young's modulus; thus, cantilevers can be made shorter while maintaining the same force constant. Processing of polymers does not require sophisticated equipment, so such probe arrays could be manufactured more cheaply. Zou et al. fabricated an array of more than 1,000,000 probes on a 7.5-cm glass slide. Tips and cantilevers made of photodefinable polyimide film were individually supported on SU-8 bonding structures; each of these structures had a footprint of 10 μm × 10 μm.

Passive pen arrays command that all pens in the array create the same pattern. Different inks must be amenable to the same environmental conditions in order to be deposited at the same time. Although they are more complicated to fabricate, active pens can create more complex structures, with multiple inks over large areas, and inks that do not necessarily deposit under the same environmental conditions can be deposited in series.

Rosner et al. [31] fabricated thermal bimorph actuators from evaporated Cr/Pt/Au on silicon nitride cantilevers. The gold thin-film resistor essentially acts as a heater and concentrates the heat away from the probe tip. When power is delivered, cantilevers are actuated in the direction normal to the heated surface. Bullen et al. [93] fabricated a similar array of ten thermal bimorph actuators, with cantilevers 300 μm long spaced 100 μm apart. Resistive heating actuates the cantilevers away from the substrate. Each cantilever was individually addressed by two lead wires. A typical actuation current of 10 mA resulted in an 8-μm deflection and an average probe temperature of 298 K above ambient. A ten-probe individually addressed, thermally actuated array of cantilevers 1400 μm long, 20 μm wide, 8 μm thick and spaced 100 μm apart was used to pattern ODT on gold substrates with sub-50-nm resolution [94]. Zou et al. [80] fabricated an array of 45 thermal bimorph probes in which cantilever alignment was achieved via contact sensing based on the detection of electrical continuity between the tips and the substrate. This required that both elements be partially or entirely conductive.

Limitations to thermal bimetallic actuation include the potential negative effects of the heat on inks such as biomolecules [95]. There may also be thermal crosstalk between probes—heat conduction and convection through the air between probes leading to unwanted tip deflection, effects which increase as the distance between probes decreases. Bullen and Liu [95] found that the smallest pitch in thermal bimetallic arrays where crosstalk was manageable was 100 μm. This led to the fabrication of an array of electrostatically actuated DPN probes with an array pitch of 30 μm (Fig. 5.17). The probes act as electrodes separated from the counter electrode, the array holder, by SU-8 photoepoxy acting as an insulator. The probes are grounded via conducting paste. Actuation occurs by applying a voltage (typically around 190 V) to the counter electrode; the probe tips are then pulled off the surface. Grounding the lithography surface ensures there is no electric field or actuator force between the tips and the substrate. While thermal crosstalk is avoided with electrostatically actuated probes, there may be crosstalk due to fringe electric fields.

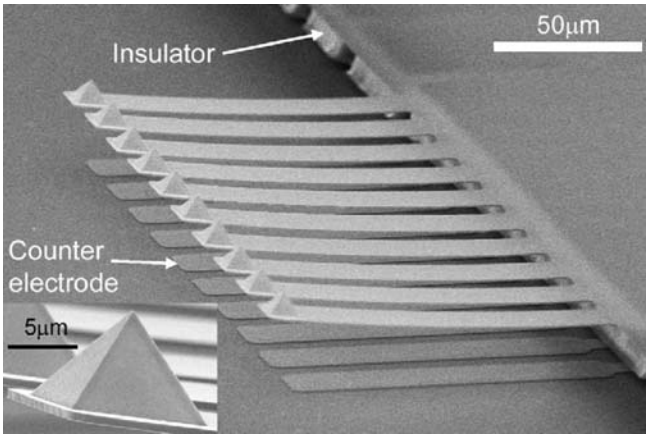

Fig. 5.17. SEM image of an electrostatically actuated DPN array [95]

Crosstalk deflection with these probes was similar to that in thermal bimetallic actuators, but at the substantially reduced array pitch of 30 μm.

A third method for probe actuation uses piezoelectric films. Lead zirconate titanate (PZT) has a high piezoelectric coefficient and can be integrated into cantilever probes. Zhu et al. [96] described a method to fabricate $50 \times 100\ \mu m^2$ microcantilevers with 1-μm-thick PZT membranes with almost 100% yield. Currently, the integration of piezoelectric bending actuators onto the NFP array is under development, and preliminary actuation results confirmed the feasibility of the operation with active probes [97]. With active probes capable of lifting the tips off the substrate, independent patterns can be made on individual writing sites, in one scanning stroke. Since scalability was proven with the one-dimensional array, the NFP is currently being augmented to a two-dimensional array with an integrated microfluidic network. This would bring the NFP one step closer to a production tool to generate, in a massively parallel fashion, templates that consist of broad range of analytes. While the augmentation to two-dimensional arrays is a matter of scalability and wafer-level-yields engineering, the operation of two-dimensional NFP arrays would require specially designed AFM systems rather than the presently available AFM instruments. With the adoption of piezoelectric precision stages or microelectromechanical system stages [98, 99], it is feasible that the two-dimensional NFP array could pattern large areas to produce multicomponent templates. In this case, leveling between the array and the substrate can be achieved with a three-probe feedback scheme, as reported for scanning probe data storage [100]. By avoiding the implementation of individual sensors on each probe, this approach can reduce the complexity of the system. With this scheme, the two-dimensional array can be maintained parallel to the substrate in the same way as an air table. Like one-dimensional arrays, passive probes are adequate if duplicate patterns, for example, nanoarrays, are to be fabricated. Alternatively, individual active probes allow the writing of different patterns with each probe.

For the operation of two-dimensional arrays of active probes with independent bending actuation, each cantilever requires one electrical connection for its electrode, assuming one set of electrodes shares the electrical path, while the others are indepen-

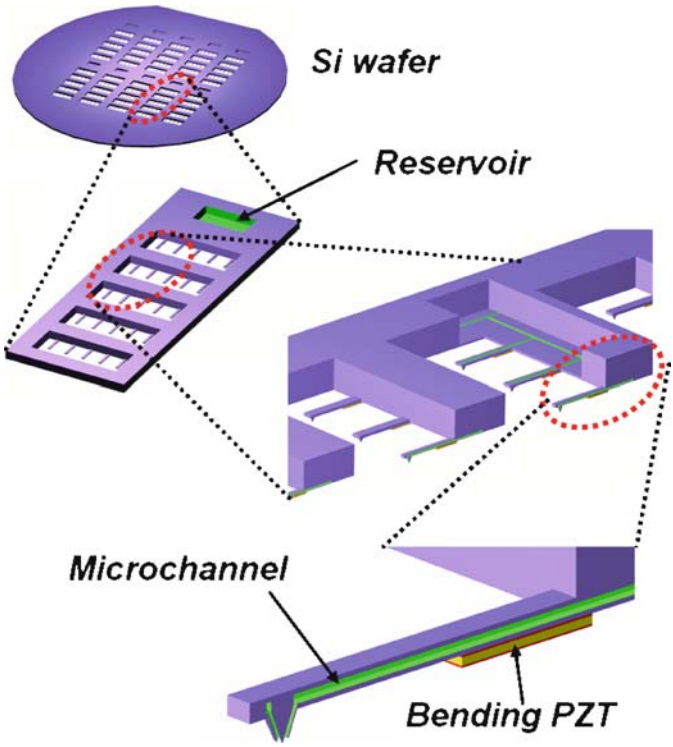

Fig. 5.18. Conceptual diagram of massively parallel NFP arrays for wafer-level patterning. *PZT* lead zirconate titanate

dently driven. Such direct drive is straightforward and simple when the size of the array is small. However, for a large array, such as a massively parallel two-dimensional array with a large number of cantilevers, a multiplexed addressing scheme needs to be employed to reduce the number of connections. This scheme is widely used in computer memories and liquid-crystal displays. Since the probe must be in continuous contact with the substrate between command signals, a bistable (memory) element must be integrated at the root of each cantilever. Furthermore, with multiple reservoirs on the wafer, individual reservoirs may contain one type of molecular ink to feed a cantilever or a group of cantilevers. Through this approach of multiple inks and massively parallel tips, NFP arrays have the potential to manufacture nanoscale features of chemical/biochemical materials at the wafer level (Fig. 5.18).

5.6 Future Prospects for Nanoprobes

Cantilevered nanoprobes offer the possibility of flexible protein deposition for diagnostic applications and drug screening. In addition to being compatible with SPM-readout methods, nanoprobe devices can be used in concert with classic pro-

tein analysis techniques such as ELISA. The probes can also deliver DNA for the purposes of genomic studies or nanoconstruction. The most recent advances in nanoprobes for biomolecule deposition involve the integration of microfluidics into cantilevers and the arraying of multiple probes in one and two dimensions. Higher-throughput patterning and a reduction in feature size have been achieved, and a better theoretical understanding of the patterning process has been acquired.

Aside from the direct and indirect patterning of biological materials, there are several other applications offered by cantilevered probes, such as in-depth studies of cell adhesion. Cells were able to adhere to DPN-generated patterns [39], although the pattern resolution was well below that of the length scale at which protein clustering in focal adhesion occurs [19]. Increasing the resolution attainable via probe-based patterning methods will improve the quality of rigid ligand templates for such studies. Controlled delivery can also be used for the study of cell communication: local perturbation of one cardiac myocyte in a small cluster of cells was achieved with the insertion of less than five α-toxin channels into the cell membrane using the nanopipette [101]. It could be observed that perturbation of one cell in a small cluster can affect the neighboring cells.

The atomic force microscope can also be exploited for its force sensitivity; it is able to measure piconewton forces associated with single molecules. In fact, AFM is currently the only force technique capable of mapping and analyzing single molecules with nanoscale lateral resolution [28]. AFM force spectroscopy involves measuring the interaction force between the AFM probe tip and the sample as the tip is pushed towards the sample and then retracted. The AFM probe deflection is measured as a function of the vertical displacement of the piezoelectric scanner. The technique can interrogate the forces and dynamics of interaction between individual ligands and receptors; this is essential to fundamental studies in molecular recognition, protein folding and unfolding, DNA mechanics and cell adhesion. The development of smaller cantilevers such as nanotube tips functionalized with single biomolecules should improve the force resolution, allowing for the measurement of smaller unbinding forces.

Finally, functionalized cantilevers may also operate as biosensors. For example, specific binding events cause changes in cantilever deflection [102]. Grogan et al. [103] demonstrated that antibody-coated cantilevers could be used to detect myoglobin concentrations in the range of normal physiological concentration in human serum. The change in frequency of a resonating cantilever can also be measured; this change is due to adsorption of biological material onto an appropriately functionalized tip. For example, Gupta et al. [104] fabricated arrays of silicon cantilever beams 20–30 nm thick to detect the mass of individual virus particles.

Cantilevered probes have the potential to enable new investigations in the life sciences, and improve diagnostic abilities in the health sciences. With continuing advancements, high-throughput assays performed rapidly and with high sensitivity are becoming a reality.

Acknowledgements. This work was supported primarily by the Nanoscale Science and Engineering Initiative of the National Science Foundation under NSF Award Number EEC–0647560. The authors acknowledge the Microfabrication Applications Laboratory of the University of Illinois at Chicago, the Cornell NanoScale Science & Technology Facility of Cornell University, the

Materials Processing and Crystal Growth Facility of Northwestern University, Northwestern University Atomic- and Nanoscale Characterization Experimental Center, and the Electron Microscopy Center of Argonne National Laboratory for the fabrication and characterization facilities.

References

1. Tang Q, Zhang Y, Chen L, Yan F, Wang R (2005) Nanotechnology 16:1062–1068
2. Wadu-Mesthrige K, Amro NA, Garno JC, Xu S, Liu G-Y (2001) Biophys J 80:1891–1899
3. Bier FF, Andresen D, Walter A (2006) In: Urban GA (ed) BioMEMS. Springer, Dordrecht, pp 167–198
4. Auburn RP, Kreil DP, Meadows LA, Fischer B, Matilla SS, Russell S (2005) Trends Biotechnol 23(7):374–379
5. Reese MO, van Dam RM et al (2003) Genome Res 13:2348–2352
6. Sotomayor Torres CM (ed) (2003) Alternative lithography: unleashing the potentials of nanotechnology. Kluwer/Plenum, Dordrecht
7. Bernard A, Renault JP, Michel B, Bosshard HR, Delamarche E (2000) Adv Mater 12(14):1067–1070
8. Hovis JS, Boxer SG (2000) Langmuir 16(3):894–897
9. Michel B, Bernard A, Bietsch A, Delamarche E, Geissler M, Juncker D, Kind H, Renault JP, Rothuizen H, Schmid H, Schmidt-Winkel P, Stutz R, Wolf H (2001) IBM J Res Dev 45(5):697–719
10. Mesquida P, Blanco EM, McKendry RA (2006) Langmuir 22(22):9089–9091
11. Tarlov MJ, Burgess DRF, Gillen G (1993) J Am Chem Soc 115(12):5305–5306
12. Lipshutz RJ, Fodot SPA, Gingeras TR, Lockhart DJ (1999) Nat Genet 21:20–24
13. Singh-Gasson S, Green RD, Yue Y, Nelson C, Blattner F, Sussman MR, Cerrina F (1999) Nat Biotechnol 17(10):974–978
14. Stoll D, Templin MF, Bachmann J, Joos TO (2006) In: Urban GA (ed) BioMEMS. Springer: Dortrecht, pp 245–268
15. Anonymous (2006) Nature 444(7121):963–964
16. Christman KL, Requa MV, Enriquez-Rios VD, Ward SC, Bradley KA, Turner KL, Maynard HD (2006) Langmuir 22(17):7444–7450
17. Pierce Biotechnology (2006) ELISA. Pierce Biotechnology, Rockford
18. Saliterman SS (2006) BioMEMS and medical microdevices. SPIE, Bellingham
19. Arnold M, Cavalcanti-Adam EA, Glass R, Blümmel J, Eck W, Kantlehner M, Kessler H, Spatz JP (2004) Chem Phys Chem 5(3):383–388
20. Ngunjiri JN, Li J-R, Garno JC (2006) In: Kumar CSSR (ed) Nanodevices for the life sciences, vol 4, 1st edn. Wiley-VCH, Weinheim pp 67–108
21. Lenhert S, Sun P, Wang Y, Fuchs H, Mirkin, Chad A (2007) Small 3(1):71–75
22. Henderson E, Lynch M, Nettikadan S, Johnson J, Huff J, Xu J, Mosher C, Vengasandra S, Radke K, Cao C, Ryckman K, Kristmundsdottir A (2004) Microsc Microanal 10:1432–1433
23. Christman KL, Enriquez-Rios VD et al (2006) Soft Matter 2:928–939
24. Lynch M, Mosher C, Huff J, Nettikadan S, Johnson J, Henderson E (2004) Proteomics 4:1695–1702
25. Lee M, Kang D-K, Yang H-K, Park K-H, Choe SY, Kang C, Chang S-I, Han MH, Kang I-C (2006) Proteomics 6(4):1094–1103
26. Yu X, Cheng DXQ (2006) Proteomics 6(20):5493–5503
27. Hu J, Zhang Y, Gao H, Li M, Hartmann U (2002) Nano Lett 2(1):55–57
28. Hinterdorfer P, Dufrene YF (2006) Nat Methods 3(5):347–355

29. Piner RD, Zhu J, Xu F, Hong S, Mirkin CA (1999) Science 283:661–663
30. Ginger DS, Zhang H, Mirkin CA (2004) Angew Chem Int Ed Engl 43(1):30–45
31. Rosner B, Duenas T, Banerjee D, Shile R, Amro N, Rendlen J (2006) Smart Mater Struct 15:S124–S130
32. Meister A, Jeney S, Liley M, Akiyama T, Staufer U, De Rooij NF, Heinzelmann H (2003) Microelectron Eng 644:67–68
33. Meister A, Liley M, Brugger J, Pugin R, Heinzelmann H (2004) Appl Phys Lett 85(25):6260–6262
34. Fang A, Dujardin E, Ondarcuhu T (2006) Nano Lett 6(10):2368–2374
35. Kim K-H, Moldovan N, Espinosa HD (2005) Small 1(6):632–635
36. Moldovan N, Kim K-H, Espinosa HD (2006) J Micromech Microeng 16:1935–1942
37. Wu B, Ho A, Moldoval N, Espinosa H (2007) Langmuir 23(17):9120–9123
38. Nafday OA, Weeks BL (2006) Langmuir 22:10912–10914
39. Lee K-B, Park S-J, Mirkin CA, Smith JC, Mrksich M (2002) Science 295:1702–1705
40. Vega RA, Maspoch D, Shen CKF, Kakkassery JJ, Chen BJ, Lamb RA, Mirkin CA (2006) Chembiochem 7(11):1653–1657
41. Lee KB, Kim EY, Mirkin CA, Wolinsky SM (2004) Nano Lett 4(10):1869–1872
42. NanoInk (2007) Protein arrays application note. NanoInk, Skokie. http://www.nanoink.net/d/appnote_protein_arrays.pdf
43. Wilson DL, Martin R, Hong S, Cronin-Golomb M, Mirkin CA, Kaplan DL (2001) Proc Natl Acad Sci USA 98(24):13660–13664
44. Lee K-B, Lim J-H, Mirkin CA (2003) J Am Chem Soc 125:5588–5589
45. Lim J-H, Ginger DS, Lee K-B, Heo J, Nam J-M, Mirkin CA (2003) Angew Chem Int Ed Engl 42(20):2309–2312
46. Nam J-M, Han SW, Lee K-B, Liu X, Ratner MA, Mirkin CA (2004) Angew Chem Int Ed Engl 43(10):1246–1249
47. Demers LM, Ginger DS, Park S-J, Li Z, Chung S-W, Mirkin CA (2002) Science 296:1836–1838
48. Zhang H, Elghanian R, Amro NA, Disawal S, Eby R (2004) Nano Lett 4(9):1649–1655
49. Agarwal G, Sowards LA, Naik RR, Stone MO (2002) J Am Chem Soc 125:580–583
50. Xu J, Lynch M, Huff JL, Mosher C, Vengasandra S, Ding G, Henderson E (2004) Biomed Microdevices 6(2):117–123
51. Vengasandra SG, Lynch M, Xu J, Henderson E (2005) Nanotechnology 16:2052–2055
52. Schena M, Heller RA, Theriault TP, Konrad K, Lachenmeier E, Davis RW (1998) Trends Biotechnol 16(7):301–306
53. Belaubre P, Guirardel M et al (2003) Appl Phys Lett 82(18):3122–3124
54. Belaubre P, Guirardel M et al (2004) Sens Actuators A 110:130–135
55. Leichle T, Silvan MM et al (2005) Nanotechnology 16(4):525
56. Saya D, Le T et al (2007) J Micromech Microeng 17(1):N1
57. Bietsch A, Zhang J, Hegner M, Lang HP, Gerber C (2004) Nanotechnology 15(8):873
58. Espinosa HD, Kim K-H, Moldovan N (2006) In: Kumar CSSR (ed) Nanodevices for the life sciences, vol 4, 1st edn. Wiley-VCH, Weinheim, pp 109–149
59. Bruckbauer A, Ying L, Rothery AM, Zhou D, Shevchuk AI, Abell C, Korchev YE, Klenerman D (2002) J Am Chem Soc 124(30):8810–8811
60. Bruckbauer A, Zhou D, Ying L, Korchev YE, Abell C, Klenerman D (2003) J Am Chem Soc 125(32):9834–9839
61. Rodolfa KT, Bruckbauer A, Zhou D, Korchev YE, Klenerman D (2005) Angew Chem Int Ed Engl 44(42):6854–6859
62. Rodolfa KT, Bruckbauer A, Zhou D, Schevchuk AI, Korchev YE, Klenerman D (2006) Nano Lett 6(2):252–257

63. Hu H, Xie S, Meng X, Jing P, Zhang M, Shen L, Zhu Z, Li M, Zhuang Q, Shao Y (2006) Anal Chem 78(19):7034–7039
64. Kim K-H, Ke C, Moldovan N, Espinosa HD (2003) In: Proceedings of the 4th international symposium on MEMS and nanotechnology. The 2003 SEM annual conference and exposition on experimental and applied mechanics, Charlotte, NC, 2–4 June, pp 235–238
65. In: Materials Research Society symposium proceedings, fall MRS meeting, 2004, p A5.56.1
66. Espinosa HD, Moldovan N, Kim K-H (2007) In: Bhushan B, Fuchs H (eds) Applied scanning probe methods, vol VII. Springer, Berlin, pp 77–134
67. Kim K-H, Sanedrin RG, Ho AM, Lee SW, Moldovan N, Mirkin CA, Espinosa HD (2007) Direct Delivery and Submicron Patterning of DNA by Nanofountain Probe. In press in Advanced Materials, 2007
68. Deladi S, Tas NR, Berenschot JW, Krijnen GJM, de Boer MJ, de Boer JH, Peter M, Elwenspoek MC (2004) Appl Phys Lett 85(22):5361–5363
69. Deladi S, Berenschot JW, Tas NR, Krijnen GJM, de Boer JH, de Boer MJ, Elwenspoek MC (2005) J Micromech Microeng 15:528–534
70. Xu S, Miller S, Laibinis PE, Liu G-Y (1999) Langmuir 15:7244–7251
71. Liu G-Y, Amro NA (2002) Proc Natl Acad Sci USA 99(8):5165–5170
72. Naujoks N, Stemmer A (2004) Colloids Surf A 249(1–3):69–72
73. Agarwal G, Naik RR, Stone MO (2003) J Am Chem Soc 125:7408–7412
74. Jang J, Hong S, Schatz GC, Ratner MA (2001) J Chem Phys 115(6):2721–2729
75. Sheehan PE, Whitman LJ (2002) Phys Rev Lett 88(15):156104
76. Cho N, Ryu S, Kim B, Schatz GC, Hong S (2006) J Chem Phys 124(2):024714
77. Weeks BL, Vaughn MW, DeYoreo JJ (2005) Langmuir 21:8096–8098
78. Rozhok S, Sun P, Piner R, Lieberman M, Mirkin CA (2004) J Phys Chem B 108(23):7814–7819
79. Weeks BL, Noy A, Miller AE, De Yoreo JJ (2002) Phys Rev Lett 88(25):255505
80. Zou J, Wang X, Bullen D, Liu C, Mirkin C (2006) Proc SPIE 6223:62230N-10
81. Hampton JR, Dameron AA, Weiss PS (2005) J Phys Chem B 109(49):23118–23120
82. Weeks BL, DeYoreo JJ (2006) J Phys Chem B 110(21):10231–10233
83. Schwartz PV (2002) Langmuir 18(10):4041–4046
84. Peterson EJ, Weeks BL, DeYoreo JJ, Schwartz PV (2004) J Phys Chem B 108(39):15206–15210
85. Nafday OA, Vaughn MW, Weeks BL (2006) J Chem Phys 125:144703
86. Manandhar P, Jang J, Schatz GC, Ratner MA, Hong S (2003) Phys Rev Lett 90(11):115505
87. Lee N-K, Hong S (2006) J Chem Phys 124(11):114711
88. Xu J, Lynch M, Nettikadan S, Mosher C, Vegasandra S, Henderson E (2006) Sens Actuators B 113(2):1034–1041
89. Lee SW, Oh BK, Sanedrin RG, Salaita K, Fujigaya T, Mirkin CA (2006) Adv Mater 18(9):1133–1136
90. Vettiger P, Despont M, Drechsler U, Durig U, Haberle W, Lutwyche MI, Rothuizen HE, Stutz R, Widmer R, Binnig GK (2000) IBM J Res Dev 44(3):323–340
91. Vettiger P, Cross G, Despont M, Drechsler U, Durig U, Gotsmann B, Haberle W, Lantz MA, Rothuizen HE, Stutz R, Binnig GK (2002) IEEE Trans Nanotechnol 1(1):39–55
92. Salaita K, Wang Y, Fragala J, Vega RA, Liu C, Mirkin CA (2006) Angew Chem Int Ed Engl 45(43):7220–7223
93. Bullen D, Chung S-W, Wang X, Zou J, Mirkin CA, Liu C (2004) Appl Phys Lett 84(5):789–791
94. Wang X, Bullen DA, Zou J, Liu C, Mirkin CA (2004) J Vac Sci Technol B 22(6):2563–2567
95. Bullen D, Liu C (2006) Sens Actuators A 125(2):504–511
96. Zhu H, Miao J, Chen B, Wang Z, Zhu W (2005) Microsyst Technol 11:1121–1126

97. Northwestern University (2007) Espinosa research group. http://clifton.mech.northwestern.edu/∼nfp/
98. Rothuizen H, Drechsler U, Genolet G, Haberle W, Lutwyche M, Stutz R, Widmer R, Vettiger P (2000) Microelectron Eng 53(1–4):509–512
99. Kim CH, Jeong HM, Jeon JU, Kim YK (2003) J Microelectromech Syst 12(4):470–478
100. Lutwyche M, Andreoli C, Binnig G, Brugger J, Drechsler U, Haberle W, Rohrer H, Rothuizen H, Vettiger P, Yaralioglu G, Quate C (1999) Sens Actuators A 73(1–2):89–94
101. Ying L, Bruckbauer A, Zhou D, Gorelik J, Shevchuk A, Lab M, Korchev Y, Klenerman D (2005) Phys Chem Chem Phys 7:2859–2866
102. Ziegler C (2004) Anal Bioanal Chem 379:946–959
103. Grogan C, Raiteri R, O'Connor GM, Glynn TJ, Cunningham V, Kane M, Charlton M, Leech D (2002) Biosens Bioelectron 17(3):201–207
104. Gupta A, Akin D, Bashir R (2004) Appl Phys Lett 84(11):1976–1978